Structure of the Complex between Phosphorylated Substrates and the SCF β-TrCP Ubiquitin Ligase Receptor: A Combined NMR, Molecular Modeling, and Docking Approach

Nathalie Evrard-Todeschi,[†] Julien Pons,[†] Josyane Gharbi-Benarous,[†] Gildas Bertho,[†] Richard Benarous,[‡] and Jean-Pierre Girault*[,†]

Laboratoire de Chimie et Biochimie Pharmacologiques et Toxicologiques, Université Paris Descartes, UMR 8601-CNRS, 45 rue des Saint-Pères, 75006 Paris, France, and Cellvir, 4 rue Pierre Fontaine, 91000 Evry, France

Received July 24, 2008

The binding of phosphorylated peptides to the receptor plays a major role in many basic cellular processes in a variety of pathological states. Human β-TrCP is a key component of a recently characterized E3 ubiquitin ligase complex that regulates protein degradation through the ubiquitin-dependent proteasome pathway. Docking studies were carried out to explore the structural requirements for the β-TrCP substrates. Docking studies were performed on the bound conformation of the phosphorylated peptides determined by NMR, whereas the β-TrCP structure was derived by X-ray from Protein Data Bank. After the docking calculation, during which the peptides were conformationally restrained, the complex presented herein was analyzed in terms of ligand-protein interactions and properties of contacting surfaces. The structural requirements for phosphorylated substrates in interaction with β-TrCP were explored and compared with experimental data from TRNOESY and STD NMR results. The analysis revealed that the bend of the peptide structures, which is indispensable for β-TrCP recognition, aligns two charged phosphate groups and a central hydrophobic group in a favorable arrangement that leads to the burial of the peptide surface in the binding cleft upon complexation. Through docking simulations, we have identified different specific binding pockets of β-TrCP according to the ligand in interaction. These data should be valuable in the rational design of a ligand to be used in therapeutic approaches.

INTRODUCTION

The ubiquitin pathway is involved in the regulation of many basic cellular processes, such as cell cycle progression, differentiation and development, and immune and inflammatory responses. The ubiquitin−proteasome system targets many regulatory proteins for rapid intracellular proteolysis. Ubiquitin is conjugated to target proteins by a stepwise cascade of E1, E2, and E3 enzymes that activate and transfer ubiquitin as a thioester linkage for ultimate transfer to a lysine residue on the substrate. Reiteration of the catalytic cycle synthesizes a ubiquitin polymer that targets the substrate to the 26S proteasome, where it is rapidly unfolded and degraded.[1−3] A diverse array of E3 enzymes, often also referred to as ubiquitin ligases, specifically recognizes one or more cognate substrates. Several classes of E3 enzymes have been described; among those there are the SCF complexes that recognize phosphorylated substrates.

These SCF complexes are composed of the linker protein Skp1, the cullin scaffold protein Cdc53, and the domain protein Rbx1/Roc1, which are common to all SCFs, and a variable F-box protein.[4,5] F-box proteins contain a Skp1-binding site called the F-box and a substrate interaction domain, such as a WD40 repeat domain or a leucine rich repeat (LRR) domain that appears to be responsible for specific recognition of phosphorylated substrates (Figure 1A).[6,7]

The first identification of human β-TrCP (beta-transducin repeat-containing protein) was made as the F-box receptor component of the E3 ubiquitin ligase SCF- β-TrCP responsible for the degradation of CD4 induced by the human immunodeficiency virus type 1 (HIV-1) protein Vpu.[8] Subsequently, SCF-β-TrCP is also responsible for phosphorylation-dependent ubiquitination and then for the degradation of IκB-α, β-catenin, and ATF4 (Figure 1B).[9−14]

It is commonly thought that IκB-α is subsequently ubiquitinated and degraded in the cytoplasm, resulting in NF-κB nuclear translocation and transcription stimulation of target genes.[15] Similarly, it is also thought that β-catenin ubiquitination and subsequent degradation take place in the cytoplasm, preventing nuclear translocation of the protein which is required for TCF/LEF transcriptional activation of target genes responsible for inflammatory responses.[16] The F-box protein β-TrCP is colocalized in the nucleus with ATF4, a member of the ATF-CREB bZIP family of transcription factors, and controls its stability. ATF4 plays a crucial role in response to stress.[17−20] In addition, ATF4 is important for cell proliferation and differentiation[21,22] and is a critical regulator of osteoblast differentiation, function,[23] and bone resorption.[24]

The β-TrCP binding process plays a key role in a variety of pathological states and therefore has been the target of numerous studies. Preliminary results on mapping the binding

* Corresponding author phone: 33-1-42-86-21-80; fax: 33-1-42-86-83-87; e-mail: jean-pierre.girault@parisdescartes.fr.
[†] Université Paris Descartes.
[‡] Cellvir.

10.1021/ci800248u CCC: $40.75
Published on Web 11/20/2008

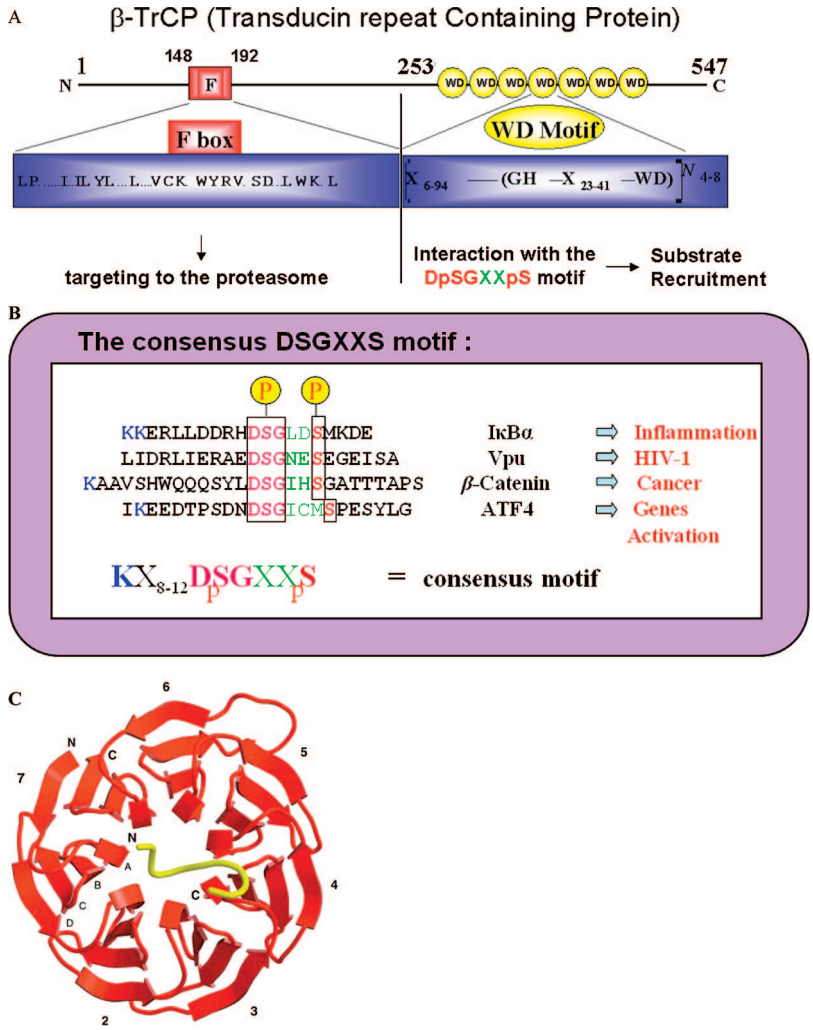

Figure 1. Scheme of the β-TrCP protein structures according to the crystal structure[34] of the human β-TrCP-Skp1 complex bound to a β-catenin peptide. *A*) The diagram of β-TrCP shows the F box responsible for proteasome targeting through Skp1 binding and the seven WD-40 repeats involved in binding substrates. *B*) The phosphorylation site containing the consensus motif D**pS**G*XX***pS** is shown in four peptide ligands of the β-TrCP protein. *C*) The phosphorylated β-catenin peptide binds to the top of the WD40 domain of β-TrCP, and it partially dips into the central channel. The seven blades of the WD40 domain are numbered from 1 to 7, and the strands within each blade are conventionally named A to D.

Table 1. Sequence Peptide Ligands of the β-TrCP Protein[a]

name	sequence number	sequence	source
11P-β-catenin	30−40	YL**DSGIHS**GAT	X-ray
23P-ATF4	208−230	IKEEDTPSDN**DSGICMS**PESYLG	NMR[b]
24P−IκBα	21−44	KKERLLDDRH**DSGLDS**MKDEEYEQ	NMR[b]
22P-Vpu	41−62	LIDRLIERAE**DSGNES**EGEISA	NMR[b]

[a] Structures used for binding mode prediction. [b] NMR, minimized average structure.

epitope of β-TrCP ligands have already been published.[25−28] Vpu, IκB-α, and β-catenin have been shown to share a common phosphorylated motif, D**pS**G*XX***pS**, while ATF4 has a similar but slightly different motif, D**pS**G*XXX***pS** (Figure 1B). Both motifs are required for interaction with β-TrCP.

Here, the structural β-TrCP complex data collected to date are enhanced by experimental data. NMR studies using transfer NOE techniques and saturation transfer difference NMR (STD NMR) have been established as important techniques to identify binding activities and to characterize binding epitope of ligands with atomic resolution.[29−31]

Finally, a comparison with previous NMR and crystallographic results complements our understanding of the respective β-TrCP binding reactions.

Molecular docking plays an important role in structure-based drug design.[32,33] Ligand docking starting from NMR bound conformers, presented in Table 1 (22P-Vpu, 32P-β-catenin, 24P-IκBα, and 23P-ATF4), is essential to predict ligand binding modes and to consider the β-TrCP protein structural variations in ligand binding. For these complexes, only the 11P-β-catenin/β-TrCP X-ray structure[34] is available, whereas all NMR bound structures determined in solution are available for studying ligand docking into the β-TrCP protein binding site. In the first docking stage, we started from the structure initially derived from the X-ray complex β-TrCP protein bound to a ligand 11P-β-catenin peptide[34] (Figure 1C) and substituted 11P-β-catenin by ligand NMR conformations in the β-TrCP binding site. To examine the

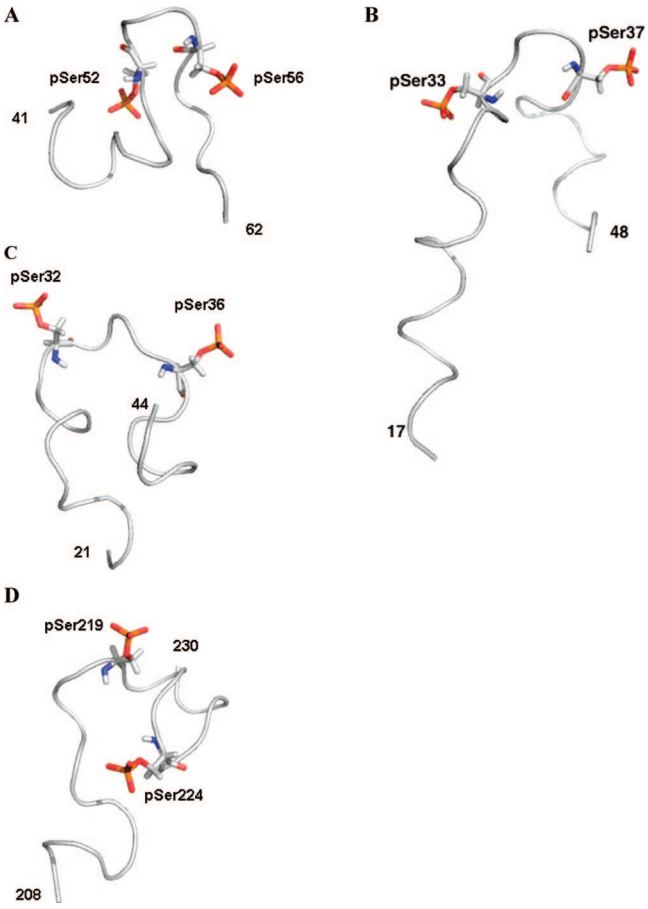

Figure 2. The NMR TRNOE-derived structure of the different bound peptides in the presence of the MBP-β-TrCP protein was generated with ARIA software, and the minimum energy-minimized conformer with best fit of proton distance constraints was shown: *A*) 22P-Vpu, *B*) 32P-β-catenin, *C*) 24P-IκBα, and *D*) 23P-ATF4.

interaction mechanism of various ligands on the β-TrCP receptor, we studied the possible binding modes in a 3D model of the β-TrCP-peptide models of ATF4, Vpu, IκB-α, and NMR entity of β-catenin. The four peptides were taken in their putative NMR binding conformations (Figure 2) and were then respectively superimposed to 11P-β-catenin in the X-ray model. The docked complex revealed key features for the interaction and structural requirements for the conformation of β-TrCP substrates.

MATERIALS AND METHODS

Materials. *Peptides.* HIV-1 encoded virus protein U (Vpu) fragment (41−62), β-catenin fragment (17−48), IκB-α fragment (21−44), and ATF4 fragment (208−230), hereafter referred to as peptides 22P-Vpu, 32P-β-Cat, 24P-IκBα, and 23P-ATF4, respectively, were purchased from NeoMPS Laboratory, Strasbourg (France). The peptides were N-acylated and C-amidated at their respective termini. The purity (95%) of the peptides was tested by analytical HPLC and by mass spectrometry. The amino acid sequences for the peptides of several β-TrCP ligands including Vpu, IκBα, β-catenin, and ATF4 are reported in Table 1.

Purification of the WD Repeat Region from Human Protein β-TrCP Fused to the Maltose Binding Protein (MBP). Coding sequence corresponding to the 253−547 residues of full-length protein β-TrCP was inserted into the pMAL-C2X expression vector (OZYME). The construction resulted in a fusion protein of approximately 75 kDa corresponding to the 361 residues of the MBP,[35] a 33-mer linker and the seven WD repeats (residues 253−547) of β-TrCP, hereafter named MBP-β-TrCP.[27] Protein concentration was determined using the standard Bradford method following the optical density at 595 nm. Finally, the purified recombinant protein was concentrated and dialyzed in the NMR buffer in order to remove maltose. Following this protocol, the final yield of purified MBP-β-TrCP was of 3.5 mg/L. This amount of purified recombinant protein was used to prepare the NMR samples.

NMR Experiments.[27,36] The experiments were run at 500.13 MHz for ^{1}H on a Bruker Avance 500 NMR spectrometer (Bruker Biospin, Wissembourg, France) equipped with an ^{1}H, ^{13}C, ^{15}N TXI probe, and a Linux workstation, using sample tubes with a 5-mm outer diameter. Two-dimensional NMR spectra were recorded in the phase-sensitive mode using the States-TPPI method.[37] All experiments were carried out using the WATERGATE pulse sequence for water suppression[38] or using the excitation sculpting water suppression[39] to eliminate the solvent signal in $H_2O/^2H_2O$ (95:5) solution. The following conventional two-dimensional experiments TOCSY,[40] and NOESY,[41] and ROESY[42] spectra and the 2D heteronuclear experiments, ^{1}H−^{13}C HSQC,[43] ^{1}H−^{13}C HSQC with multiplicity editing during selection step[44] and ^{1}H−^{13}C HMBC[45] were recorded at 280 K in the 50 mM sodium phosphate buffer at pH 7.2. Spectra were processed using XWIN-NMR 3.5 (Bruker Biospin, France) and analyzed with FELIX (Accelrys, France) software.

NMR Spectroscopy of Ligand-Protein Interaction. The NMR sample of peptide in the presence of β-TrCP contained 20 μM protein and 2 mM peptide, for a ratio of 100:1 peptide:protein binding sites, in PBS solution, 50 mM (NaH_2PO_4/Na_2HPO_4), pH 7.2, containing 0.02% NaN_3 and 5% ^2H_2O.

STD is a very sensitive method that allows the mapping of binding epitopes.[30,31] Saturation of a single target resonance can result in a rapid spread of saturation over the entire macromolecule if spin diffusion within the macromolecule is efficient. The ligand resonances also become saturated provided that the ligand protons are close in space to the macromolecular protons. The one-dimensional STD-NMR spectra of β-TrCP/peptide were recorded with selective saturation of protein resonances with on-resonance irradiation at 11 ppm or −1 ppm and off-resonance irradiation at 30 ppm for reference spectra. The 1D STD spectra were obtained by internal subtraction of saturated spectra from reference spectra by phase cycling.

The STD experiments can be used in a qualitative way to detect if a known ligand is displaced in the presence of other NMR substrates that are then regarded as inhibitors. Indeed a competition STD NMR experiment indirectly allows the detection of the higher affinity ligand by monitoring the STD signals of the 32P-β-catenin ligand in the P-peptide/32P-β-catenin mixture on the β-TrCP protein.[46]

Titration WaterLOGSY enables the evaluation of the dissociation binding constant.[46] The detail of the pulse sequence version used for WaterLOGSY experiment can be found in the literature.[27,36]

Transferred nuclear Overhauser effect (TRNOESY)[47,48] spectra of β-TrCP/peptides were recorded with a mixing time of 150 ms. Automatic baseline correction was performed prior to the integration of cross-peak volumes, using FELIX (Accelrys, France). Cross-peak intensities were converted to distances[49] by using the distance between two H aromatic protons (2.43 Å) as a reference. The TRNOE cross−peak intensities were classified as strong (1.8−2.7 Å), medium (1.8−3.6 Å), and weak (1.8−5.0 Å).

Methods of Computation. *Three-Dimensional Structure Calculation.* Structure calculations were based on TRNOESY spectra of β-TrCP/peptides. The calculated distances were incorporated into ARIA 1.2 simulated annealing protocol running within the program CNS[50,51] for molecular dynamics calculations using the PARALLHDG 5.3 force field. During the calculations, non-glycine residues were restrained to negative φ values (usually the only range considered in NMR-derived structures).[52] ARIA enabled the incorporation of ambiguous distance restraints and calibration of the NOE restraints using automated matrix analysis as implemented by the program.[53] ARIA runs were performed using the default parameters with eight iterations. In the final iteration, a set of lowest-energy structures was retained as final structures. The set of peptide structures was selected for correct geometry, and no distance restraint violations of >0.5 Å. Analysis of the structures was performed within AQUA, PROCHECK-NMR programs.[54] MOLMOL[55] was used for the analysis and presentation of the results of the structure determination. Finally, 10 structures were chosen to represent the conformation of the peptide that is consistent with NMR data.

Docking. For the different docking experiments, the structure of the β-TrCP protein (PDB code 1P22) was extracted from the Protein Data Bank in readable PDB format [Research Collaboratory for Structural Bioinformatics (RSCB) (http://www.rscb.org/pdb)]. All calculations were performed using the Sybyl 7.3 molecular modeling program package (Tripos Inc., France) running under the RedHat Enterprise operating system on a PC workstation.

Docking simulations were carried out using the Surflex-Dock program.[56] The Surflex-Dock 2.0 is a fully flexible molecular docking algorithm that combines the scoring function of the Hammerhead docking system and a patented search engine to dock ligands into a protein binding site.[57] It uses a computational representation of the intended binding site called protomol.[58] The protomol is built from the hydrogen-containing protein mol2 file. The protein surface is coated with three types of probes that represent potential hydrogen bond (C═O and N−H are respectively the hydrogen bond acceptor and donor probe) and favorable hydrophobic interactions with protein atoms (CH_4 is the steric hydrophobic probe). For each ligand, the Hammerhead procedure is as follows: (1) generate the ligand fragment in order to reduce the conformational space that must be explored, (2) align the fragments onto the protomol probes, and (3) dock the remainder of the ligand fragments. A full molecule is then positioned from the aligned fragment and scored using an empirically derived function that includes charged and hydrogen bond polar terms, solvation, and entropic and hydrophobic complementary terms. Surflex-Dock scores[59] are expressed in -log(K_d) units to represent binding affinities. During the docking procedure, the β-TrCP protein frame was fixed, whereas all peptide fragments were allowed to move. The starting peptide conformations were derived from NMR data. In all cases the N-terminus was calculated in its protonated positively charged state and the C-terminal carboxyl group in its negatively charged state. The ligand fragments have a large number of charged residues. The experimental populations change with pH. Of course, the docking can only implicitly take the pH into account when working on the protonated or nonprotonated species favored at pH 7.2, the NMR experimental pH (NH_3^+, CO_2^-, and PO_3^{2-}). After setting the protonation state, 11P-β-catenine, 11P-Vpu, IκBα, and ATF4 have respectively a total charge of −4, −9, −5, and −7. A set of complex structures was generated and analyzed with regard to energy terms, intramolecular and intermolecular interactions, buried surface area, and stereochemical quality. The buried surface was defined by contacting atoms at the complex interfaces and was analyzed with regard to STD-NMR data. The interactions shown were those mediated by hydrogen bonds and by hydrophobic contacts. We used the HBPLUS[60] program for calculating these different contacts for plotting by Ligplot.[61]

RESULTS AND DISCUSSION

The SCF-β-TrCP complex specifically recognizes a Vpu peptide fragment of 22 amino acids, the 22P-Vpu peptide (viral protein of HIV-1);[25] a 32 residue β-catenin polypeptide, the 32P-β-catenin (oncogenic protein);[26] a 24 amino acid motif in IκB-α, the 24P-IκBα (chronic inflammatory pathologies);[28] and a 23P-ATF4 peptide derived from the human ATF4 protein (transcription factor).[27] The NMR method allows the determination of the binding epitopes of these different ligands. The interaction of the substrates, Vpu, IκB-α, β-catenin, and ATF4 with β-TrCP, relies on a similar motif, D**pS**G*XX(X)***pS**.

Determination of β-TrCP/Peptide Equilibrium Constants K_d. The dissociation constant for the interaction of the phosphorylated peptides to the MBP-β-TrCP protein was measured by NMR. WaterLOGSY represents a powerful method for primary NMR screening in the identification of compounds that interact with macromolecules. The method is particularly useful for the evaluation of the dissociation binding constant.[46] The dissociation binding constants K_d are characteristic of fast exchange condition, 23P-ATF4, K_d = 500 μM, 32P-β-catenin, K_d = 1000 μM, 22P-Vpu, K_d = 200 μM, 24P-IκBα, K_d = 400 μM, at 280 K. This range of binding affinity makes the peptide likely to be suitable for TRNOESY NMR experiments that require fast exchange between the free and bound states.

Peptide Structure. TRNOESY experiments[47,48] were used to investigate the bound conformation of the peptide. The complexes between the phosphorylated peptides and the β-TrCP protein consisting of the N-terminal F box domain (residues 139 to 186), a C-terminal WD40-repeat domain (residues 253 to 545), and an α-helical domain (residues 187 to 252, the linker domain) that links the two domains, were investigated by means of 2D-TOCSY and 2D-TRNOESY experiments. The spectroscopic investigation yielded distance constraints for the peptide conformation (Table 2). The NMR-derived interproton distances were applied as distance constraints in simulated annealing calculations. The observed

Table 2. Structural Statistics of the Final NMR Structures of the Ligands Bound to the β-TrCP Protein

	β-catenin	Vpu	IκBα	ATF4
no. of exptl distance restraints				
unambiguous NOE	350	183	313	224
ambiguous NOE	105	38	4	92
total NOEs	455	221	317	316
divided into				
intraresidue NOE	213		166	150
sequential NOE	150		92	113
medium range NOE	85		36	40
long range NOE	7		23	13
no. of exptl broad dihedral restraints	28	18	21	20
NOE violations >0.3 Å per structure	1.6	5	0.5	0.4
Rmsd[a] (Å) to a mean molecule				
backbone (all residues)	5.6 ± 1.9	2.0 ± 0.9	1.33 ± 0.38	1.9 ± 0.6
heavy atoms (all residues)	6.0 ± 1.7	3.3 ± 1.1	2.63 ± 0.63	2.7 ± 0.7
backbone (motif residues)	2.0 ± 0.9	0.15 ± 0.07	0.63 ± 0.29	1.7 ± 0.6
heavy atoms (motif residues)	2.4 ± 0.8	0.13 ± 0.06	1.68 ± 0.48	2.5 ± 0.6
Ramachandran plot of residues[b] (%)				
in most favored regions	35.2	45	52	38.9
in additional allowed regions	57.0	28	44	55.6
in generously allowed regions	7.4	27	4	5.6
in disallowed regions	0.4	0	0	0.0

[a] Calculated by MOLMOL. [b] Calculated by PROCHECK.

peptide structures were characterized by an N-terminal loop followed by a large bend centered on the doubly phosphorylated destruction motif D**pS**G*XX***pS** (Figure 2). The bound 22P-Vpu showed a structured helical N-terminal part, residues 43−49, and a large bend ED**pS**^{52}GNE**pS**^{56}E, from residue Glu50 to residue Glu57 (Figure 2A). For β-catenin, two regions of the peptide seem to be required for the interaction with the β-TrCP: the ^{32}D**pS**G*XX***pS**^{37} phosphorylated motif and a helical region, located just before the phosphorylated motif ^{24}HWQQQ^{28} (Figure 2B). The structure of the bound 24P-IκBα is composed of a well-defined bend between residues His30 and pSer36, ^{31}D**pS**GLD**pS**MK^{38}. Moreover, the bend is flanked by two turn Lys22−Asp31 and Met37−Tyr42 regions (Figure 2C). Only the large bend D**pS**GICM**pS** of 23P-ATF4 comprises two opposite loops, Ser^{215}-Ile^{221} and Ile^{221}-Ser^{227}, respectively, in the calculated structure (Figure 2D).

These bound structures would expose the hydrophobic side chain (Leu or Ile) in the center and the two phosphorylated Ser (**pSer**) side chains implemented in the bend for interactions with the β-TrCP protein, a hypothesis consistent with the STD-NMR data. This is very likely induced by the shape of the β-TrCP binding channel, that forces the peptide backbones to adopt a tighter turn compared to the one of the free state. In conclusion, it can be stated that the phosphorylated peptides are prestructured ligands in solution showing a characteristic bend in their hairpin loop structures.

X-ray β-TrCP/11P-β-Catenin Complex. The F box protein β-TrCP recognizes the doubly phosphorylated D**pS**G*XX***pS** destruction motif, present in Vpu, β-catenin, and IκBα, and directs the SCF-β-TrCP to ubiquitinate these proteins at specific lysines. The structure of the β-TrCP protein, extracted from the Protein Data Bank consists of the N-terminal F box domain (residues 139 to 186), a C-terminal WD40-repeat domain (residues 253 to 545), and an α-helical domain (residues 187 to 252, the linker domain) that links the two domains.[34] The seven WD40 repeats form a torus-like structure (named β propeller) that has a narrow channel running through its middle. The 11P-β-catenin peptide binds to the top face of the β propeller, opposite from where the linker packs to the F-box protein. In the crystal structure, only a segment of 11 residues (residues 30 to 40), centered on the doubly phosphorylated destruction motif (residues 32 to 37), is ordered in the structure. The phosphoserine, aspartic acid, and hydrophobic residues of the motif are recognized directly by contacts from β-TrCP. The β-catenin peptide binds the top face of the β propeller with the six residues motif that dips into the central channel.

To date, only one crystal structure of β-TrCP in complex with a ligand (11P-β-catenin) has been reported. The consensus emerging from various substrates/β-TrCP complex studies and the X-ray crystallography structure of β-catenin/β-TrCP is that the binding of β-TrCP is due to the seven WD-40 repeats. Hence, the crystal structure can be utilized to extrapolate the interaction of other substrates (Figure 3).

Validation of the Docking Method. To ensure that conformation and orientation of the ligand obtained from the docking studies were likely to represent valid and reasonable binding modes of the different β-TrCP substrates, the Surflex-Dock program docking parameters first had to be validated for the crystal structure used 11P-β-catenin/β-TrCP. To do so, the 11P-β-catenin ligand, in the conformation found in the crystal structure (Figure 3B), was extracted and docked back into the corresponding binding pocket to determine the ability of Surflex-Dock to reproduce the orientation and the position of this substrate. Surflex-Dock employs an idealized active site ligand called a protomol,[58] as a target to generate putative poses of molecules or molecular fragments. These putative poses are scored using the Hammerhead scoring function,[59] which also serves as an objective function for local optimization of poses. The definition of the protomol is a sensitive step, and the docking performance depends on the area considered to form the binding site. The binding pockets can be defined either from a cocrystallized ligand (L) or from a list of residues (R) known to be part of the interaction site. Two parameters (Threshold and Bloat) needed to be tailored in order to determine the extent of the protomol and adapted to a binding

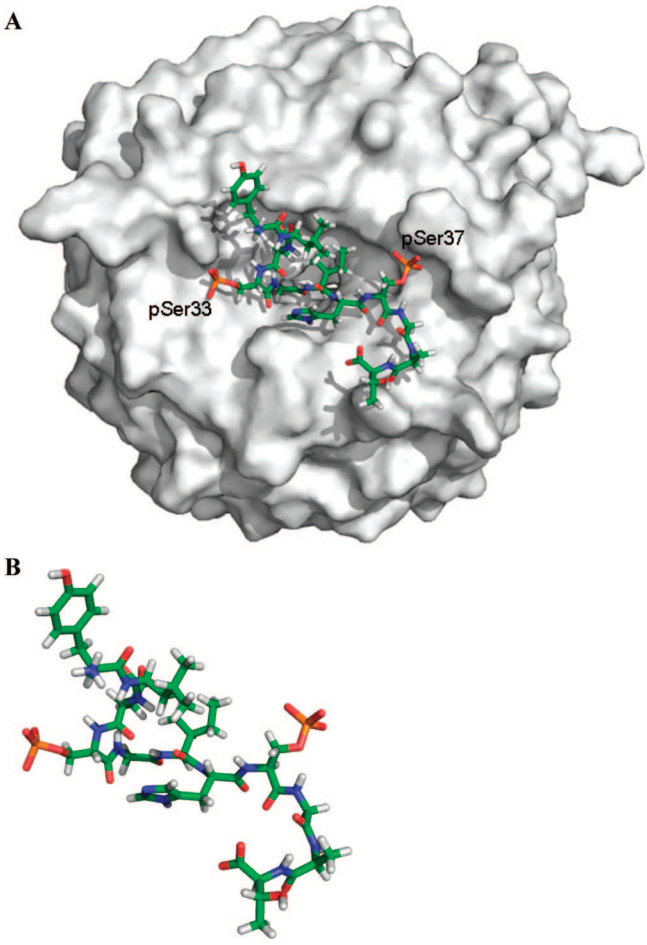

Figure 3. According to the crystal structure[34] of the human β-TrCP-Skp1 complex bound to a β-catenin peptide: *A*) Surface representation of the top face of the β-TrCP WD40 domain with the bound 11P-β-catenin peptide. *B*) The diphosphorylated 11P-β-catenin YLD**pS**GIH**pS**GAT motif, where both phosphate groups of **pSer** are shown, points out the structure bound to the β-TrCP protein.

pocket. Threshold value (proto-thresh) is a factor that determines to what extent the protomol can be buried in the protein; increasing this number will decrease the volume (default 0.5). The bloat value (proto-bloat) can be used to inflate the protomol and includes nearby crevices (default 0).

Considering that the protein structure included a ligand and that the construction of the protomol was based on the position of the said ligand, we have used different values of proto-thresh (0.2; 0.3; 0.4; and 0.5) coupled with two values of proto-bloat (0 and 1).

We constructed eight different protomols named for example L-0.2-0 (L for ligand, proto-thresh=0.2, and proto-bloat=0). For each docking, we obtained thirty poses listed in descending order of score values. The results of the docking with the eight different protomols are summarized in Table 3. The docking accuracy was evaluated in terms of the root means square deviation (rmsd) between the docked position and the experimentally determined position for the ligand. For each protomol, we reported the structure with the best score (always denoted 0), with the best rmsd, and with the best RMSDiso. The docked structures were compared to the 11P-β-catenin X-ray structure according to the conformation (rmsd) and to the orientation in the active site (RMSDiso). Figure 4 shows the superimposition of the 11P-

Table 3. Characteristics of the Various Protomols According to the Construction Mode

		RUN		
protomol	ranking	score	RMSDiso	rmsd
	0[a]	2.9	8.9	4.0
L-0.2-0	2[b]	2.3	6.6	3.5
	4[c]	1.1	9.1	2.7
	0	6.2	8.9	3.2
L-0.2-1	19	3.0	7.2	2.8
	19	3.0	7.2	2.8
L-0.3-0	0	10.5	15.1	4.1
	8	3.5	11.5	3.6
	6	4.5	13.1	2.7
L-0.3-1	*0*	*8.5*	*3.3*	*1.8*
	10	*5.1*	*3.1*	*2.2*
	10	*5.1*	*3.1*	*2.2*
L-0.4-0	0	10.0	14.0	1.7
	22	2.5	11.7	3.0
	7	4.8	14.3	1.7
L-0.4-1	*0*	*12.0*	*5.8*	*2.6*
	25	*5.9*	*3.7*	*1.9*
	25	*5.9*	*3.7*	*1.9*
L-0.5-0	*0*	*8.2*	*4.4*	*2.0*
	13	*2.7*	*3.3*	*1.6*
	13	*2.7*	*3.3*	*1.6*
L-0.5-1	0	6.2	10.9	3.5
	2	5.4	9.0	4.7
	4	3.3	11.7	2.8

[a] Structure with the best score. [b] Structure with the best RMSDiso. [c] Structure with the best rmsd calculated with all atoms.

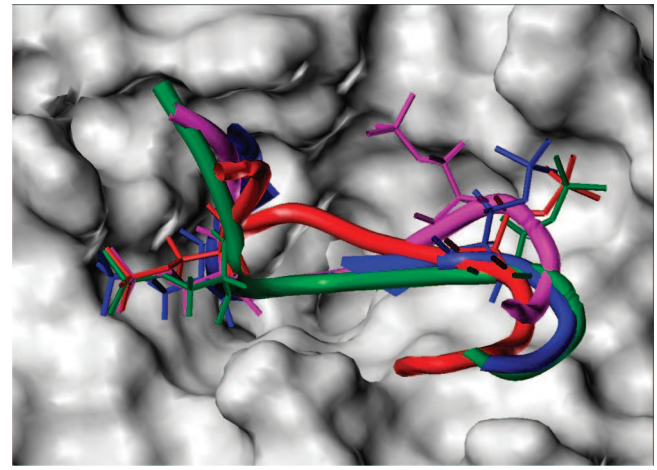

Figure 4. Superposition of the 11P-β-catenin crystal structure (*blue*) and the docked structures with the best RMSDiso according to the construction of protomol: L-0.3-1 (*green*), L-0.4-1 (*red*), and L-0.5-0 *(magenta)*.

β-catenin crystal structure (blue) and of the docked structures with the best RMSDiso according to the construction of protomols: L-0.3-1 (green), L-0.4-1 (red), and L-0.5-0 (magenta).

Figure 4 shows that the positions of the two phosphorylated pSer are in identical relative position except for the structure obtained with proto-tresh=0.5, proto-bloat=0 in magenta. Moreover, the low rmsd (3.6 Å) and low RMSDiso (3.1 Å) between the docked structure obtained with the L-0.3-1 protomol and crystal ligand coordinates indicate very good alignment of the experimental and calculated positions. We can observe the same largest number of contacts, hydrogen bonds, and electrostatic interactions between β-TrCP and the crystal structure of the doubly phosphory-

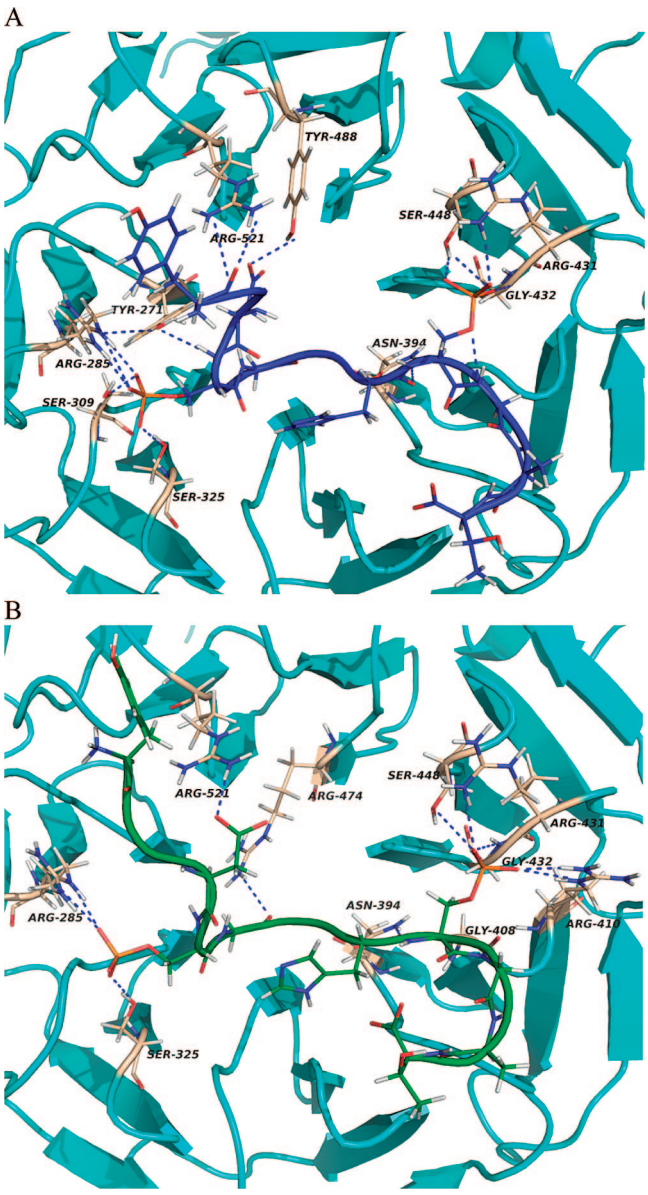

Figure 5. Close-up view of the interface between the β-TrCP WD40 domain and A) the crystal structure of the doubly phosphorylated 11P-β-catenin peptide (in blue) and *B*) the docked structure with the L-0.3-1 protomol (in green). Hydrogen bonds are represented by yellow dotted lines.

lated 11P-β-catenin peptide (Figure 5A), as between β-TrCP and the docked structure with the L-0.3-1 protomol (Figure 5B). The phosphate group of the first **pSer** in the D**pS**G*XX***pS** motif makes hydrogen bonds with side chain hydroxyl groups of Ser325 and electrostatic interactions with the guanidinium group of Arg285. The phosphate group of the second **pSer** contacts fewer residues, forming hydrogen bonds with the hydroxyl group of Ser448 and the backbone amide group of Gly432 and electrostatic interactions with the guanidinium group of Arg431. Thus, protomol L-0.3-1 (proto-thresh=0.3 and proto-bloat=1) was used for docking studies of the three substrates: Vpu, IκB-α, and ATF4.

Docking of the NMR Structures with *β*-TrCP. Computational docking of proteins involves different issues such as location of the binding site, packing of irregular objects, and evaluation of surface complementarity. It has been shown that the prediction of binding site structures yielded correct results when 'directed modeling' was applied.[62] The β-TrCP binding site is formed by a channel that runs through the middle of the WD40 β propeller structure with a hydrophobic pocket and positively charged residues at the top face of the β propeller, thus presenting potential locations for hydrogen bonds to the peptide ligand. For docking calculations, the ligand was placed near this putative binding site. When using the Surflex-Dock program, the docking routine generated randomized ligand-β-TrCP protein assemblies. The β-TrCP protein was constrained in mobility, but peptides were not. This allowed sampling of the conformational space toward induced fit shapes. Approximations were introduced into the docking routine by defining peptide backbone NMR and by fixing the β-TrCP protein framework. The complex structures found were stereochemically plausible, with respect to their steric arrangements and their interactions, and therefore supported our results. Docking calculations were performed in the absence of solvent molecules, and therefore energy contributions of the burial of hydrophobic side chains in the binding site were presumably underestimated. However, each of the most frequently found complex geometries reflected a putative conformation, and the one that was finally chosen was in accordance with the experimental NMR bound structure.

Different ligands induce different binding mode prediction. From the bound NMR structure of the different ligands, a segment of 11 residues, centered on the doubly phosphorylated destruction motif, was taken into account as for the 11P-β-catenin X-ray structure (Figure 5). The ligand, *via* the bound NMR energy-minimized structure, was cross-docked into the β-TrCP crystal structure originally bound with another ligand (11P-β-catenin). The NMR ligand structures were superimposed by matching 15 backbone atoms in the binding site (the D**pS**G*XX* fragment). Figures 6−9 show the result of β-TrCP-receptor docking against the NMR minimized structure of the bound peptides.

Contacts and Bonds. Table 4 summarizes the hydrogen bond contacts for the four β-TrCP ligands after the docking studies.

Epitope of the β-Catenin Peptide. The structure of β-catenin exhibits an N-terminal domain with a tendency to form turns followed by a bend and its C-terminal flexible part (Figure 6A-1). The β-catenin peptide binds to the top face of the β-TrCP WD domain. The majority of different **pSer** contacts, hydrogen bond, and electrostatic interactions are located in two W1−W2 and W4−W5 domains. pSer33 makes contact with Arg285 (W1) and Ser325 (W2), and pSer37 with Arg410 (W4), Arg431 (W5), Ser448 (W5). These contacts are reinforced by Asp32, which interacts with Arg521 (W7), His36 with Asn394 (W4), and Gly38 with Gly408 (W4).

All NH of the ^{32}D**pS**GIH**pS**G^{38} motif interact strongly with the corresponding amino acids inside the site. Gly34 and Ile35 are able to make hydrophobic interactions with a hydrophobic pocket (Leu351 and Ala434, Asn394 respectively) of the β-TrCP channel. These contacts could participate in increasing the affinity of the binding region.

The STD results are also consistent with the conformational epitope obtained by docking. To describe the region responsible for the binding interaction of the P-peptides with β-TrCP, specific affinity was investigated by STD NMR spectroscopy experiments.[29,31] STD NMR spectroscopy offers an efficient alternative approach to identify the residues

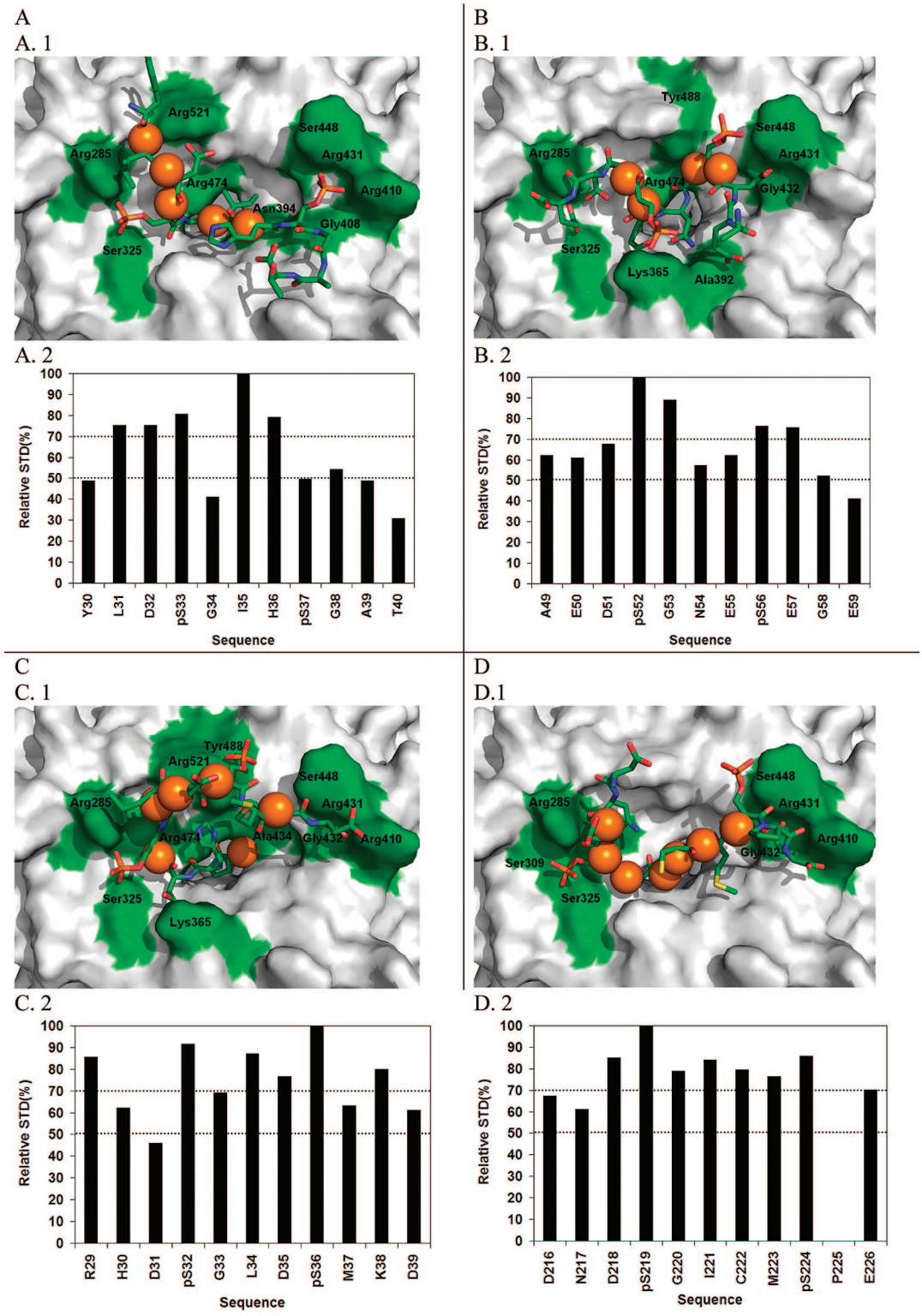

Figure 6. Results of docking studies starting with the NMR bound structure of the four peptides for *A*) β-catenin, *B*) Vpu, *C*) IκB-α, and *D*) ATF4, respectively. *1*) β-TrCP is shown in surface representation, the different contacts, hydrogen bonds, and electrostatic interaction between the peptide are represented in green. The different peptide structures after docking are represented in stick format with the side chains. STD results have been added to the docked structure: the amide protons with the strongest STD amplification factor are displayed as *colored spheres*: *orange* for the strongest (>70%). *2*) Relative STD intensities for the peptides centered on the D**pS**GXX**pS** motif. The integral value of the largest signal was set to 100%. The relative degree of saturation for the individual protons normalized to that of the largest signal can be used to compare the STD effect.

involved in binding to receptor proteins. Comparison of the STD spectra demonstrated the involvement of the NH groups of the residue sequence D**pS**G*XX***pS** (or D**pS**G*XXX***pS**) in binding. Two groups of residues seem to be important for β-catenin binding and, therefore, should be closer to the protein surface than the other protons (Figure S1).[26] The first one is the group of residues of the ^{31}LD**pS**GIH**pS**^{37} motif (including Leu31), and the second is that of the 24−28 region. The STD spectrum of the 11P-β-catenin clearly demonstrated the involvement of the HN of residues such

Table 4. Results of the Docking Studies Starting with the NMR Bound Structure (β-catenin, Vpu, IκB-α, and ATF4)[a]

β-TrCP		β-catenine						Vpu										IKBα								ATF4					
		D32	pS33	G34	H36	pS37	G38	E50	D51	pS52	G53	N54	E55	pS56	E57	G58	E59	R29	H30	D31	pS32	G33	pS36	K38	D39	N217	D218	pS219	pS224	P225	E226
W1	Y271																				X					X					
	R285		X												X	X	X				X						X	X			
W2	S309																											X			
	S325		X												X		X				X							X			
W3	K365												X	X						X											
W4	A392							X																							
	N394				X																										
	G408						X																								
	R410					X																			X					X	X
W5	R431					X			X	X															X				X		
	G432								X																X						X
	A434																	X													
	S448					X			X																						X
W6	R474			X							X	X						X	X												
	Y488										X													X							
W7	R521	X																				X	X								

[a] The **X**s correspond to the hydrogen bonds [calculated by the HBPLUS program for plotting Ligplot] observed between the amino acids of the ligand and the residues of seven WD repeats of β-TrCP.

as Leu31, Asp32, pSer33, Ile35, and His 36 which have similar larger STD intensities, ranging from 70% to 100% (Figure 6A-2).

Epitope of the Vpu Peptide. The bound 11P-Vpu peptide showed a bend corresponding to the **pS**^{52}GNE**pS**^{56} motif and two turn regions on both sides (Ala49-Asp51 and Glu57-Glu59). The overall negative potential generated by the five aspartic and glutamic acid residues increases with the phosphorylated pSer52 and pSer56. The Asp51, Ser-(PO_3^{2-})52, Glu55, Ser(PO_3^{2-})56, Glu57, and Glu59 residues form a negative surface and thus provide a plausible binding region. Thus, in the bound 11P-Vpu peptide, the negative electrostatic potential dominates the peptide surface completely. The first motif D**pS**^{52}GN interacts with the W5−W6 region (Figure 6A-2−1). The phosphate group of the first phosphoserine can carry out different contacts, by forming hydrogen bonds with Arg431 (W5). Asp51 is also able to make an extensive contact because its side chain allows a hydrogen bond with Arg431, Gly432, and Ser448 (W5). Gly53 also participates in binding contacts by creating a hydrogen bond network with Arg474 and Tyr488 (W6). These W6 binding contacts are reinforced with the interaction between Asn54 and the guanidinium group of Arg474. For the second fragment E**pS**^{56}EGE, we observe the same contact with the W1−W2 domain as with β-catenin. Indeed Glu57, Gly58, and Glu59 make important contacts with Arg285 (W1) and Ser325 (W2). However the bend observed in the bound structure allows an additional contact for the second phosphorylated serine pSer56 with Lys365 (W3), reinforced with the Glu55. In the 11P-Vpu, all the strongest interactions are dominated by electrostatic interactions with the guanidinium group of Arg285 (W1), Arg431 (W5), Arg474 (W6), and NϵH of the Lys365 (W3).

The binding fragment was studied by STD-NMR spectroscopy (Figure 6A-2-2). Interaction of HIV-1 Vpu with β-TrCP relies on the phosphorylated motif ^{51}D**pS**GNE**pS**^{56} similar to that found in the other substrates of β-TrCP. The pSer52 residue gives intensive STD signals corresponding to a tight contact to protein. Strong STD signals are also observed for Gly53, Asn54, and pSer56, which are weakly bound, resulting in smaller integrals. The Glu50, Asp51, Ser(PO_3^{2-})52, Glu55, Ser(PO_3^{2-})56, and Glu57 residues form a negative surface that provides a plausible binding region. A six amino acid upstream of the phosphoserine motif, the ^{44}RLIER^{48} motif, is also implied in the interaction with β-TrCP (Figure S1). The main chain position of Ile46 and Leu45 probably lies in close proximity to a hydrophobic pocket. Signals of Leu45, Ile46, and Arg48 are also of high intensity, while the amide proton and the chain protons of Ile60, Ser61, and Ala62 are invisible. It could be shown that apart from the diphosphorylated segment (51−56), other groups in close proximity (44−48) were also involved in binding. Obviously, pSer52 and Ile46 get more saturation from the protein than the remaining residues of the ligand and therefore have more and tighter contacts to the β-TrCP's surface.

Epitope of the IκB-α Peptide. The 24P-IκBα bound NMR structure presents a bend corresponding to the ^{31}D**pS**-GLD**pS**^{36} motif with two turn regions on both sides (Lys22-Asp31 and Met37-Glu43). The turn region was stabilized by intramolecular hydrogen bounds involving Arg24, Asp27, Asp28, Arg29, His30, and Asp31 (Figure 6C-1). The side chains adopt a preferential orientation in the backbone. A hydrophilic face contained the positively charged amino acids (Lys21, Lys22, Arg24, Arg29, and His30), and the opposite hydrophilic face presented the negatively charged (Asp39, Glu40, Glu41, Glu43) and polar (Tyr42, Gln44) amino acids. The bend shows in an alternate way, the negatively charged Asp31 and pSer32, the hydrophobic residues Gly33 and Leu34, the negatively charged Asp35 and pSer36, and the hydrophobic residue Met37.

The docking results for the 11P-IκBα have revealed that the first serine pSer32 makes the same interaction as β-catenin (Figure 6C-1). The first phosphoserine pSer32 is able to make an electrostatic interaction with the positive Arg285 (W1) and hydrogen bonds with the hydroxyl groups of Tyr271 (W1) and Ser325 (W2). The second W4−W5 interaction domain is observed with the Asp39 which makes hydrogen bonds with Arg410 (W4), Arg431 (W5), and Gly432 (W5). The W6−W7 domain is also recognized in the binding mode. Indeed Arg49 and His30 make different contacts, by forming hydrogen bonds with Arg474 (W6). The phosphate group of pSer36 and Lys38 makes hydrogen bonds with Arg521 (W7) and Tyr488 (W6), respectively.

In the STD-NMR studies of the IκB-α peptide (Figure 6C-2) in the presence of β-TrCP strong enhancements were

observed for amide protons of two similar ^{31}D**pS**GLD**pS**^{36} and ^{35}D**pS**MKD**E**^{40} motifs (>60%). However, amide protons at the ^{26}LDDRH^{30} fragment have similar larger STD intensities, ranging from 50% to 80%, which indicates that these side chains are also involved in the epitope (Figure S1). The STD results highlight the binding of three motifs with the negatively charged sequences shown to play a significant role in the stabilization of the complex: the phosphorylated D**pS**^{32}GLD**pS**^{36} motif and fragments implying residue Glu (E), D**pS**^{36}MKD**E**^{40}, or D**E**^{40}EY**E**^{43}. In addition, the STD enhancements of the NH in fragment ^{25}LLDDRH^{30} show that hydrophobic Leu26 residue along with charged (Asp27, Asp28, Arg29, His30) amino acids contact the site. The relative similarity in STD effect (STD intensities between 50% and 100%) clearly shows that these different regions bind strongly to the receptor protein. The N- (^{25}LLDDRH^{30}) and C- (^{35}D**pS**MKD**E**^{40}) terminal turn regions are clearly important here as shown by the epitope mapping data (STD NMR). The fact that these residues were close to the known D**pS**GL*D***pS** binding fragment enhanced the interaction of the IκB-α ligand to the β-TrCP protein.

Epitope of the ATF4 Peptide. The ATF4 bound structure presents a well-defined turnlike structure particularly in Ser215 to pSer224, where a loop (Ile221-Tyr228) consecutive to a first turn (Ser215-Ile221) was apparent. The middle portion of the ATF4 peptide has an S-turnlike conformation (Figure 6D-1) that allows the side chain of Ile221 to insert the farthest into the channel, as in the β-catenin/β-TrCP crystal structure, making intermolecular contacts. Ile221 lies at the turning point between the two major NDpS, pSPE structure areas, thus dockings of the β-TrCP-phosphorylated ATF4 complex select the exact positioning of the Ile221 methyl tail that dips into the narrow central channel as a clip linkage leading to its stabilization. These similarities point to the central channel as a structural scaffold that can adapt, through hydrophobic side chain, to recognizing diverse secondary structures and sequences. These findings support the stucture-based conclusion that ND**pS**, **pS**PE, and Ile221 are critical for β-TrCP-ATF4 binding and specificity.

For the ATF4 ligand, the docking results highlight the binding of the N^{217}D**pS**^{219} and **pS**^{224}PE^{226} motifs (Figure 6D-1) shown to play a significant role in the stabilization of the complex. The first fragment ^{217}ND**pS**^{219} interacts with the W1−W2 domain of β-TrCP, pSer219 makes a number of contacts with Arg285 (W1), Ser309, and Ser325 (W2), while Asn217 and Asp218 make hydrogen bonds with Tyr271 (W1) and Arg285 (W1), respectively. The second pSer224 makes contact with the Arg431 (W5); moreover the Glu226 residues have the same interaction with Arg431 Gly432, and Ser448 (W5) as the second pSer of β-catenin. Ile221 with a central position in the D**pS**GICM**pS** motif could reflect its particular role as in the study of the interaction of β-catenin with β-TrCP: Ile221 is able to make hydrophobic interactions with a hydrophobic pocket (Leu351, Asn394, Ile433, Ala434, Leu472, and Arg474) in the β-TrCP channel. These contacts could participate to increasing indirectly the affinity of the binding region.

The STD-NMR results are also consistent with the conformational epitope obtained by docking (Figure 6D-2). The STD-NMR shows strong enhancements, ranging from 70% to 100%, for amide protons of the ^{218}D**pS**GICM**pS**PE^{226} motif, which indicates that these residues are involved in epitope binding. STD-NMR data allowed determining which residues in addition to the D**pS**GICM**pS** β-TrCP recognition motif in ATF4 are important for interaction, such as the negatively charged ATF4 side chains ^{218}D**pS**G**I***XX***pS***X***E**^{226}, particularly the pSer219, pSer224, and the Glu226 residues. The fact that one Glu and one Asp were close to the pSer enhanced the negative potential generated by the phosphorylated Ser. This negative pole around the phosphate groups of the Ser reinforces the ATF4 binding to the β-TrCP protein. Indeed, a fragment composed of long negatively charged residues (pSer or Glu) and short Asp in close proximity allows the binding to the β-TrCP protein.

In conclusion, by determining the conformations of Vpu, IκB-α, and ATF4, in interaction with β-TrCP at the molecular level compared with the interaction of β-catenin, we have established that structural differences in the amino acid sequence have an impact in identifying key structural parts responsible for competitive inhibition. All seven WD40 repeats of β-TrCP contribute to contacting the different ligands. We can generally assign the main common parts of the different ligands in contact with three β-TrCP binding pockets. Although the W1−W2 β-TrCP binding domain is common to all the ligands, we could also observe important contacts with the W4−W5 domain for β-catenin, IκB-α, and ATF4. Moreover β-catenin and IκB-α have a supplementary contact with the W6−W7 region. Vpu has very specific interactions with the β-TrCP. Indeed Vpu interacts with the W5−W6 region by forming hydrogen bonds. The five aspartic and glutamic acid residues imply an overall negative potential and provide a putative binding region dominated by electrostatic interactions with the W3 domain.

With the docking simulations, we have identified different binding pockets of the β-TrCP according to the ligand in interaction. As the β-TrCP binding process plays a key role in a variety of pathological states, the knowledge of ligand binding is a key step toward the design of potent competitors that may have a therapeutic value. Moreover, these results, obtained by docking, provide the first step toward the prediction of novel active compounds. Last but not least it will be possible to apply *in silico* structured-based virtual screening technologies to search for new β-TrCP inhibitors.

Abbreviations. ATF4, Activating Transcription Factor 4; β-cat, β-catenin; β-TrCP, Transducin repeat-Containing Protein; HSQC, heteronuclear single quantum correlation; IκB-α, inhibitor of nuclear factor kappa B alpha; MBP, Maltose Binding Protein; NF-κB, nuclear factor kappa B; NOE, Nuclear Overhauser Effect; NOESY, Nuclear Overhauser Effect Spectroscopy; P-, phosphorylated peptide; PBS, phosphate-buffered saline; pS, phosphorylated serine; ROESY, rotating-frame Overhauser enhancement spectroscopy; SCF, Skp1/Cul1/F-box; STD-NMR, saturation-transfer difference NMR spectroscopy; TOCSY, total correlation spectroscopy; TPPI, time proportional phase incrementation; TRNOESY, transferred nuclear Overhauser effect spectroscopy; Vpu, HIV-1 encoded virus protein U; WATERGATE, water suppression by gradient-tailored excitation.

ACKNOWLEDGMENT

We thank Franck Dupuis and Veronique Monjardet (Tripos Inc.) for providing personal technical support. We also thank

Geneviève Arnaud-Vincent (Centre for Technical Languages, Université Paris Descartes) for her critical reading of this manuscript.

Supporting Information Available: Figures showing relative STD intensities for the NMR studied peptides. This material is available free of charge via the Internet at http://pubs.acs.org.

REFERENCES AND NOTES

(1) Ciechanover, A. The ubiquitin-proteasome pathway: on protein death and cell life. *Embo J.* **1998**, *17*, 7151–7160.
(2) Hershko, A.; Ciechanover, A. The ubiquitin system. *Annu. Rev. Biochem.* **1998**, *67*, 425–479.
(3) Laney, J. D.; Hochstrasser, M. Substrate targeting in the ubiquitin system. *Cell* **1999**, *97*, 427–430.
(4) Bai, C.; Sen, P.; Hofmann, K.; Ma, L.; Goebl, M. SKP1 connects cell cycle regulators to the ubiquitin proteolysis machinery through a novel motif, the F-Box. *Cell* **1996**, *86*, 263–274.
(5) Patton, E. E.; Willems, A. R.; Tyers, M. Combinatorial control in ubiquitin-dependent proteolysis: don't Skp the F-box hypothesis. *Trends Genet.* **1998**, *14*, 236–243.
(6) Skowyra, D.; Craig, K. L.; Tyers, M.; Elledge, S. J.; Harper, J. W. F-box proteins are receptors that recruit phosphorylated substrates to the SCF ubiquitin-ligase complex. *Cell* **1997**, *91*, 209–219.
(7) Feldman, R. M.; Correll, C. C.; Kaplan, K. B.; Deshaies, R. J. A complex of Cdc4p, Skp1p, and Cdc53p/cullin catalyzes ubiquitination of the phosphorylated CDK inhibitor Sic1p. *Cell* **1997**, *91*, 221–230.
(8) Margottin, F.; Bour, S.; Durand, H.; Selig, L.; Benichou, S. A novel human WD protein, h-betaTrCP, that interacts with HIV-1 Vpu connects CD4 to the ER degradation pathway through an F-box motif. *Mol. Cell* **1998**, *1*, 565–574.
(9) Hart, M.; Concordet, J.-P.; Lassot, I.; Albert, I.; Del los Santos, R. The F-box protein beta-TrCP associates with phosphorylated beta-catenin and regulates its activity in the cell. *Curr. Biol.* **1999**, *9*, 207–210.
(10) Kroll, M.; Margottin, F.; Kohl, A.; Renard, P.; Durand, H. Inducible degradation of IkappaBalpha by the proteasome requires interaction with the F-box protein h-betaTrCP. *J. Biol. Chem.* **1999**, *274*, 7941–7945.
(11) Latres, E.; Chiaur, D. S.; Pagano, M. The human F box protein beta-Trcp associates with the Cul1/Skp1 complex and regulates the stability of beta-catenin. *Oncogene* **1999**, *18*, 849–854.
(12) Spencer, E.; Jiang, J.; Chen, Z. J. Signal-induced ubiquitination of IkappaBalpha by the F-box protein Slimb/beta-TrCP. *Genes Dev.* **1999**, *13*, 284–294.
(13) Winston, J.; Strack, P.; Beer-Romero, P.; Chu, C.; Elledge, S. The SCFbeta-TrCP-ubiquitin ligase complex associates specifically with phosphorylated destruction motifs in IkapaBalpha and Beta-Catenin and stimulates IkapaBalpha ubiquitination in vitro. *Genes Dev.* **1999**, *13*, 270–283.
(14) Yaron, A.; Hatzubai, A.; Davis, M.; Lavon, I.; Amit, S. Identification of the receptor component of the IkappaBalpha-ubiquitin ligase. *Nature* **1998**, *396*, 590–594.
(15) Karin, M. How NF-kappaB is activated: the role of the IkappaB kinase (IKK) complex. *Oncogene* **1999**, *18*, 6867–6874.
(16) Peifer, M.; Polakis, P. Wnt signaling in oncogenesis and embryogenesis--a look outside the nucleus. *Science* **2000**, *287*, 1606–1609.
(17) Harding, H. P.; Zhang, Y.; Zeng, H.; Novoa, I.; Lu, P. D. An integrated stress response regulates amino acid metabolism and resistance to oxidative stress. *Mol. Cell* **2003**, *11*, 619–633.
(18) Rutkowski, D. T.; Kaufman, R. J. All roads lead to ATF4. *Dev. Cell* **2003**, *4*, 442–444.
(19) Lu, P. D.; Harding, H. P.; Ron, D. Translation reinitiation at alternative open reading frames regulates gene expression in an integrated stress response. *J. Cell Biol.* **2004**, *167*, 27–33.
(20) Vattem, K. M.; Wek, R. C. Reinitiation involving upstream ORFs regulates ATF4 mRNA translation in mammalian cells. *Proc. Natl. Acad. Sci. U.S.A.* **2004**, *101*, 11269–11274.
(21) Tanaka, T.; Tsujimura, T.; Takeda, K.; Sugihara, A.; Maekawa, A. Targeted disruption of ATF4 discloses its essential role in the formation of eye lens fibres. *Genes Cells* **1998**, *3*, 801–810.
(22) Masuoka, H. C.; Townes, T. M. Targeted disruption of the activating transcription factor 4 gene results in severe fetal anemia in mice. *Blood* **2002**, *99*, 736–745.
(23) Yang, X.; Matsuda, K.; Bialek, P.; Jacquot, S.; Masuoka, H. C. ATF4 is a substrate of RSK2 and an essential regulator of osteoblast biology; implication for Coffin-Lowry Syndrome. *Cell* **2004**, *117*, 387–398.
(24) Elefteriou, F.; Ahn, J. D.; Takeda, S.; Starbuck, M.; Yang, X. Leptin regulation of bone resorption by the sympathetic nervous system and CART. *Nature* **2005**, *434*, 514–520.
(25) Coadou, G.; Gharbi-Benarous, J.; Megy, S.; Bertho, G.; Evrard-Todeschi, N. NMR Studies of the Phosphorylation Motif of the HIV-1 Protein Vpu Bound to the F-Box Protein β-TrCP. *Biochemistry* **2003**, *42*, 14741–14751.
(26) Megy, S.; Bertho, G.; Gharbi-Benarous, J.; Evrard-Todeschi, N.; Coadou, G. STD and TRNOESY NMR Studies on the conformation of the oncogenic protein b-Catenin containing the phosphorylated motif DpSGXXpS bound to the b-TrCP protein. *J. Biol. Chem.* **2005**, *280*, 29107–29116.
(27) Pons, J.; Evrard-Todeschi, N.; Bertho, G.; Gharbi-Benarous, J.; Tanchou, V. Transfer-NMR and Docking Studies Identify the Binding of the Peptide Derived from Activating Transcription Factor 4 to Protein Ubiquitin Ligase beta-TrCP. Competition STD NMR with beta-catenin. *Biochemistry* **2008**, *47*, 14–29.
(28) Pons, J.; Evrard-Todeschi, N.; Bertho, G.; Gharbi-Benarous, J.; Sonois, V. Structural studies on 24P-IκBα peptide derived from a human IκB-α protein-related with the inhibition of the transcription factor nuclear NFkB activity. *Biochemistry* **2007**, *46*, 2958–2972.
(29) Klein, J.; Meinecke, R.; Mayer, M.; Meyer, B. Detecting binding affinity to immobilized receptor proteins in compound libraries by HR-MAS STD NMR. *J. Am. Chem. Soc.* **1999**, *121*, 5336–5337.
(30) Mayer, M.; Meyer, B. Group epitope mapping by saturation transfer difference NMR to identify segments of a ligand in direct contact with a protein receptor. *J. Am. Chem. Soc.* **2001**, *123*, 6108–6117.
(31) Mayer, M.; Meyer, B. Characterization of ligand binding by saturation transfer difference NMR spectroscopy. *Angew. Chem., Int. Ed.* **1999**, *38*, 1784–1788.
(32) Shoichet, B. K.; McGovern, S. L.; Wei, B.; Irwin, J. J. Lead discovery using molecular docking. *Curr. Opin. Chem. Biol.* **2002**, *6*, 439–446.
(33) Halperin, I.; Ma, B.; Wolfson, H.; Nussinov, R. Principles of docking: An overview of search algorithms and a guide to scoring functions. *Proteins* **2002**, *47*, 409–443.
(34) Wu, G.; Xu, G.; Schulman, B. A.; Jeffrey, P. D.; Harper, J. W. Structure of a beta-TrCP1-Skp1-beta-catenin complex: destruction motif binding and lysine specificity of the SCF(beta-TrCP1) ubiquitin ligase. *Mol. Cell* **2003**, *11*, 1445–1456.
(35) Nallamsetty, S.; Austin, B. P.; Penrose, K. J.; Waugh, D. S. Gateway vectors for the production of combinatorially-tagged His6-MBP fusion proteins in the cytoplasm and periplasm of Escherichia coli. *Protein Sci.* **2005**, *14*, 2964–2971.
(36) Dalvit, C.; Fogliatto, G.; Stewart, A.; Veronesi, M.; Stockman, B. WaterLOGSY as a method for primary NMR screening: practical aspects and range of applicability. *J. Biomol. NMR* **2001**, *21*, 349–359.
(37) Marion, D.; Ikura, M.; Tschudin, R.; Bax, A. Rapid Recording of 2d Nmr-Spectra without Phase Cycling - Application to the Study of Hydrogen-Exchange in Proteins. *J. Magn. Reson.* **1989**, *85*, 393–399.
(38) Piotto, M.; Saudek, V.; Sklenar, V. Gradient-tailored exitation for single-quantum NMR spectroscopy of aqueous solutions. *J. Biomol. NMR* **1992**, *2*, 661–665.
(39) Hwang, T. L.; Shaka, A. J. Water Suppression That Works - Excitation Sculpting Using Arbitrary Wave-Forms and Pulsed-Field Gradients. *J. Magn. Reson. A* **1995**, *112*, 275–279.
(40) Braunschweiler, L.; Ernst, R. R. Coherence transfer by isotropic mixing: application to proton correlation spectroscopy. *J. Magn. Reson. B* **1983**, *53*, 521–528.
(41) Kumar, A.; Ernst, R. R.; Wüthrich, K. A two-dimensional nuclear Overhauser enhancement (2D NOE) experiment for the elucidation of complete proton-proton cross-relaxation networks in biological macromolecules. *Biochem. Biophys. Res. Commun.* **1980**, *95*, 1–6.
(42) Bothnerby, A. A.; Stephens, R. L.; Lee, J. M.; Warren, C. D.; Jeanloz, R. W. Structure Determination of a Tetrasaccharide - Transient Nuclear Overhauser Effects in the Rotating Frame. *J. Am. Chem. Soc.* **1984**, *106*, 811–813.
(43) Bodenhausen, G.; Ruben, D. J. Natural Abundance N-15 Nmr by Enhanced Heteronuclear Spectroscopy. *Chem. Phys. Lett.* **1980**, *69*, 185–189.
(44) Willker, W.; Leibfritz, D.; Kerssebaum, R.; Bermel, W. Gradient Selection in Inverse Heteronuclear Correlation Spectroscopy. *Magn. Reson. Chem.* **1993**, *31*, 287–292.
(45) Bax, A.; Summers, M. F. 1H and 13C assignments from sensitivity-enhanced detection of heteronuclear multi-bond connectivity by 2D multiple quantum NMR. *J. Am. Chem. Soc.* **1986**, *108*, 2093–2094.
(46) Wang, Y. S.; Liu, D.; Wyss, D. F. Competition STD NMR for the detection of high-affinity ligands and NMR-based screening. *Magn. Reson. Chem.* **2004**, *42*, 485–489.
(47) Clore, G. M.; Gronenborn, A. M. Theory and Applications of the Transferred Nuclear Overhauser Effect to the Study of the Conformations of Small Ligands Bounds to Proteins. *J. Magn. Reson.* **1982**, *48*, 402–417.

(48) Clore, G. M.; Gronenborn, A. M. Theory of the Time Dependent Transferred Nuclear Overhauser Effect: Applications to Structural Analysis of Ligand-Protein Complexes in Solution. *J. Magn. Reson.* **1983**, *53*, 423–442.
(49) Brünger, A. *X-PLOR manual*; Yale University Press: New Haven, 1993.
(50) Brünger, A. T.; Adams, P. D.; Clore, G. M.; Gros, P.; Grosse-Kunstleve, R. W. Crystallography & NMR system (CNS): A new software system for macromolecular structure determination. *Acta Crystallogr., Sect. D: Biol. Crystallogr.* **1998**, *D54*, 905–921.
(51) Linge, J. P.; Habeck, M.; Rieping, W.; Nilges, M. ARIA: automated assignment and NMR structure calculation. *Bioinformatics* **2003**, *19*, 315–316.
(52) Schibli, D. J.; Montelaro, R. C.; Vogel, H. J. The Membrane-Proximal Tryptophan-Rich Region of the HIV Glycoprotein, gp41, Forms a Well-Defined Helix in Dodecylphosphocholine Micelles. *Biochemistry* **2001**, *40*, 9570–9578.
(53) Linge, J. P.; O'Donoghue, S. I.; Nilges, M. Automated assignment of ambiguous nuclear overhauser effects with ARIA. *Methods Enzymol.* **2001**, *339*, 71–90.
(54) Laskowski, R. A.; Rullmann, J. A. C.; MacArthur, M. W.; Kaptein, R.; Thornton, J. M. AQUA and PROCHECK-NMR: programs for checking the quality of protein structures solved by NMR. *J. Biomol. NMR* **1996**, *8*, 477–486.
(55) Koradi, R.; Billeter, M.; Wüthrich, K. MOLMOL: a program for display and analysis of macromolecular structures. *J. Mol. Graph.* **1996**, *14*, 51–55.
(56) Jain, A. N. Surflex: fully automatic flexible molecular docking using a molecular similarity-based search engine. *J. Med. Chem.* **2003**, *46*, 499–511.
(57) Welch, W.; Ruppert, J.; Jain, A. N. Hammerhead: fast, fully automated docking of flexible ligands to protein binding sites. *Chem. Biol.* **1996**, *3*, 449–462.
(58) Ruppert, J.; Welch, W.; Jain, A. N. Automatic identification and representation of protein binding sites for molecular docking. *Protein Sci.* **1997**, *6*, 524–533.
(59) Jain, A. N. Scoring noncovalent protein-ligand interactions: A continuous differentiable function tuned to compute binding affinities. *J. Comput.-Aided Mol. Des.* **1996**, *10*, 427–440.
(60) Mcdonald, I. K.; Thornton, J. M. Satisfying Hydrogen-Bonding Potential in Proteins. *J. Mol. Biol.* **1994**, *238*, 777–793.
(61) Wallace, A. C.; Laskowski, R. A.; Thornton, J. M. Ligplot - a Program to Generate Schematic Diagrams of Protein Ligand Interactions. *Protein Eng.* **1995**, *8*, 127–134.
(62) Essen, L. O.; Skerra, A. The De-Novo Design of an Antibody Combining Site - Crystallographic Analysis of the V-L Domain Confirms the Structural Model. *J. Mol. Biol.* **1994**, *238*, 226–244.

CI800248U